

## CHARACTERIZATION OF COPPER-COBALT FERRITES FOR HUMIDITY SENSOR APPLICATION

Aye Aye Lwin<sup>1</sup> & Win Kyaw<sup>2</sup>

### Abstract

Nanosized Copper-Cobalt ferrites with the general formula  $\text{Cu}_x\text{Co}_{1-x}\text{Fe}_2\text{O}_4$  (where  $x = 0.00 - 1.00$  with the step of 0.25) were prepared by auto-combustion method using Analytical Reagent (AR) grade Copper Nitrate,  $\text{Cu}(\text{NO}_3)_2$ , Cobalt Nitrate Hexahydrate,  $\text{Co}(\text{NO}_3)_2 \cdot 6\text{H}_2\text{O}$  and Ferric Nitrate Nonahydrate,  $\text{Fe}(\text{NO}_3)_3 \cdot 9\text{H}_2\text{O}$ . The samples were firstly characterized by X-ray diffraction to examine the crystal structure. The average crystallite sizes were estimated from line broadening of the collected XRD patterns to determine the nanosized ferrites. Microstructural characteristics of grain shape, grain size and homogeneity of the samples were examined by Scanning Electron Microscopy (SEM). It was found that the grain shapes of the samples varied from block shape to stone-like shape with the contents  $x$  of Cu. The grain size, generally, of  $x = 0.50$  was the largest one among the investigated samples. For the applications of humidity sensors, the samples were made into circular shape pellets and the variations of the electrical resistance with the corresponding humidity range were studied in this work.

**Keywords:**  $\text{Cu}_x\text{Co}_{1-x}\text{Fe}_2\text{O}_4$ , auto-combustion method, XRD, SEM, humidity sensors.

### Introduction

The hunt for new applications of nanostructured systems is now a major area of research in materials science and technology. To exploit the full potential that nano-systems offer, it is important that novel methods of manipulation and fabrication be developed, in addition to extending current techniques of sample characterization to smaller sizes. Success in devising and assembling systems on the scale of nanometers will require a deeper understanding of the basic processes and phenomena involved. Hence, one of the current key objectives is to adapt and develop a range of techniques that can characterize the structural, electronic, magnetic and optical properties of nanostructured systems.

Humidity measurement is one of the most significant issues in various areas of applications such as instrumentation, automated systems, agriculture and climatology. In recent years improvements in sensor manufacturing technologies have occurred driven by post-process high-speed, low-power and low-cost microelectronic hybrid circuits, modern signal conditioning methods and advances in miniaturization technologies.

This work deals with the preparation of Copper-Cobalt ferrites,  $\text{Cu}_x\text{Co}_{1-x}\text{Fe}_2\text{O}_4$  (where  $x = 0.00 - 1.00$  with the step of 0.25) using auto-combustion method and their structural and microstructural characteristics were reported by XRD and SEM. For the applications of humidity sensing materials, the samples were made into pellets and their electrical resistances were investigated in the humidity range of 50 RH% – 99 RH%.

---

<sup>1</sup> Dr, Associate Professor, Department of Physics, Loikaw University

<sup>2</sup> Dr, Associate Professor, Department of Physics, Pyay University

## Experimental Details

### Preparation of the Samples

For the preparation of desired materials of Copper-Cobalt ferrites,  $\text{Cu}_x\text{Co}_{1-x}\text{Fe}_2\text{O}_4$  (where  $x = 0.00 - 1.00$  with the step of 0.25), Analytical Reagent (AR) grade Copper Nitrate,  $\text{Cu}(\text{NO}_3)_2$ , Cobalt Nitrate Hexahydrate,  $\text{Co}(\text{NO}_3)_2 \cdot 6\text{H}_2\text{O}$  and Ferric Nitrate Nonahydrate,  $\text{Fe}(\text{NO}_3)_3 \cdot 9\text{H}_2\text{O}$  were used as the starting materials. Citric Acid,  $\text{C}_6\text{H}_8\text{O}_7 \cdot \text{H}_2\text{O}$  was used as the fuel. Desired stoichiometric compositions of these Nitrates and Citric Acid were mixed with (1:1) ratio and prepared the aqueous solutions. The pH of the solution was adjusted to 7 using liquor Ammonia.

The obtained solution was allowed to evaporate in a beaker by keeping the solution temperature at  $80^\circ\text{C} - 90^\circ\text{C}$  and it was a viscous gel. The resultant gel was heated at  $450^\circ\text{C}$  for 2 h. Photographs of the weighed starting materials, as-burnt and as-prepared samples of  $\text{Cu}_x\text{Co}_{1-x}\text{Fe}_2\text{O}_4$  for  $x = 1.00$  sample are shown in Figures 1(a – c). Flow diagram of the sample preparation process is shown in Figure 2.



**Figure 1** Photographs of (a) the weighed starting materials and (b) as-burnt  $\text{Cu}_x\text{Co}_{1-x}\text{Fe}_2\text{O}_4$  for  $x = 1.00$



**Figure 1** (c) Photograph of as-burnt  $\text{Cu}_x\text{Co}_{1-x}\text{Fe}_2\text{O}_4$  for  $x = 1.00$

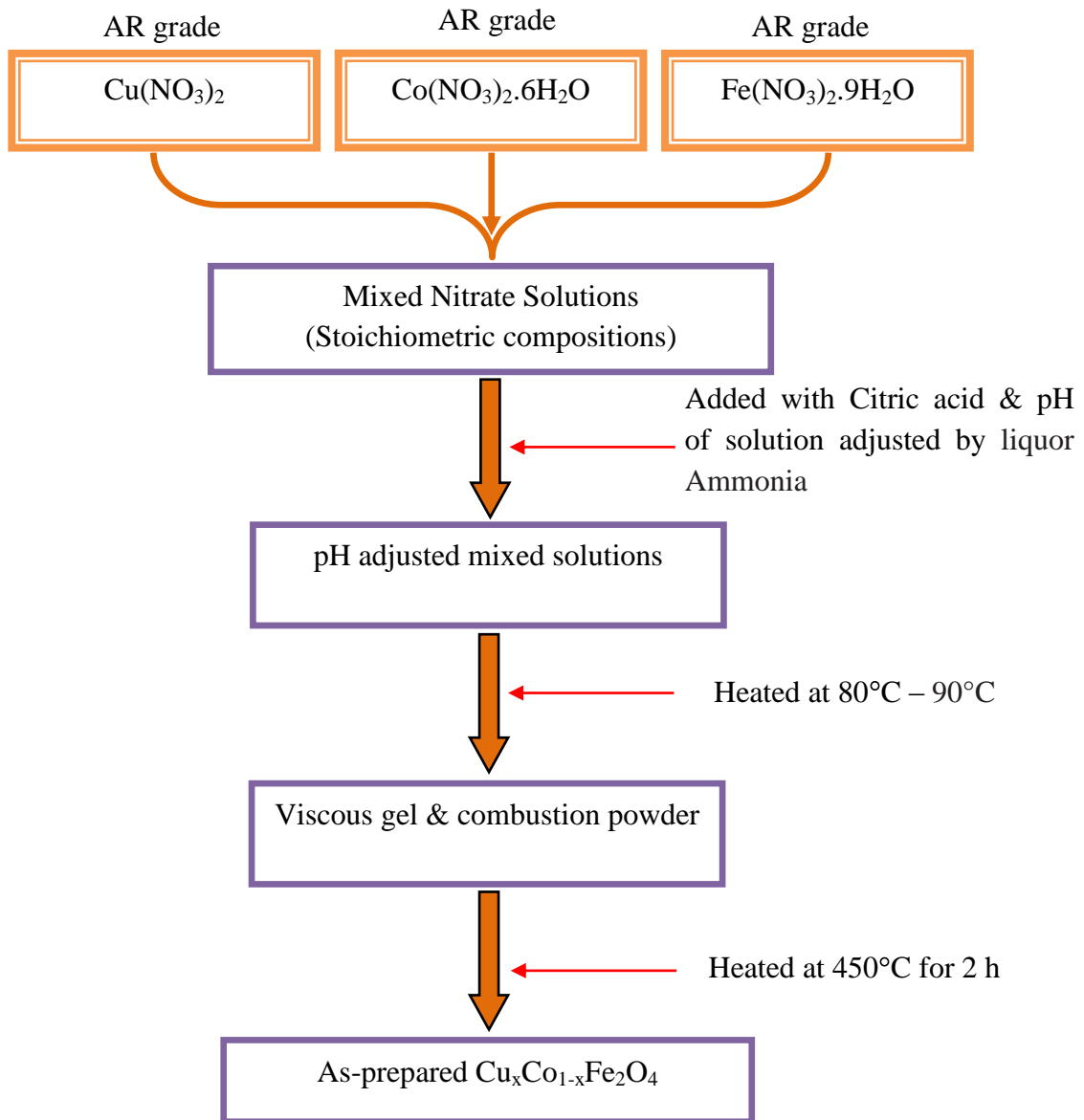


**Figure 2** Flow-diagram of the  $\text{Cu}_x\text{Co}_{1-x}\text{Fe}_2\text{O}_4$  sample preparation process

### XRD and SEM Measurements

To investigate the phase formation, structure analysis, variation of lattice parameters and estimation of crystallite sizes, the samples were characterized by XRD. Powder XRD patterns of the samples were observed by using PC-controlled RIGAKU, MULTIFLEX X-ray Diffractometer [Universities' Research Centre (URC), University of Yangon]. To examine the grain shape, grain sizes and pore formation, the samples were characterized by using JEOL JSM-5610LV SEM [Universities' Research Centre (URC), University of Yangon] with the accelerating voltage of 15 kV and 5500 times of photo magnification.

### Humidity Sensitive Electrical Resistance Measurement

For the applications of humidity sensors, the as-prepared ferrites were firstly made into circular shape pellets by using SPECAC hydraulic pellet-maker with the pressure 5 ton (~70 MPa). Thickness and area of the each of the sample were as 2.95 mm and  $1.14 \times 10^{-4} \text{ m}^2$

respectively. Silver paste was used for ensure good electrical contact. Copper ring electrodes were used to observe the resistance of the sample. In this measurement, XSW TDK 0302 Humidity Meter was used as the humidity sensing element. Humidity sensitive electrical resistances were observed in the relative humidity range of 50 RH% - 99 RH% by two probe method using FLUKE 189 digital multimeter. The refrigerator (Haier) was used as the humidity generator. Photographs of the experimental setup of humidity sensitive electrical resistance measurement are shown in Figures 3(a) and (b). Figure 4 shows the schematic diagram of the humidity sensitive electrical resistance measurement.



**Figure 3** Experimental setup of humidity sensitive electrical resistance measurements, (a) the sample and sensor placed in the same condition (altitude) and (b) wiring connection of sample and resistance meter

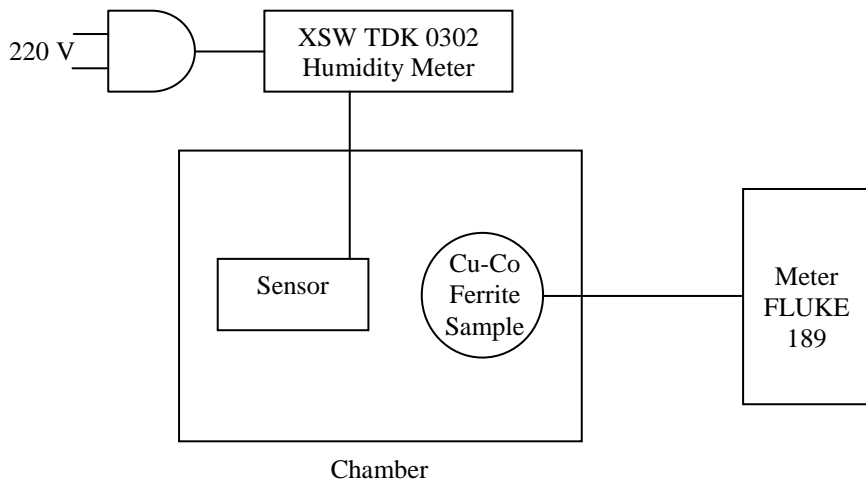


**Figure 4** Schematic diagram of the humidity sensitive electrical resistance measurement

## Results and Discussion

### XRD Study

The indexed powder X-ray diffraction patterns are shown in Figures 5(a – e). The collected XRD lines were identified by using the following JCPDS data files:

- (i) Cat. No. 22-1086>CoFe<sub>2</sub>O<sub>4</sub> – Cobalt Iron Oxide for x = 0.00 sample
- (ii) Cat. No. 22-1086>CoFe<sub>2</sub>O<sub>4</sub> – Cobalt Iron Oxide and Cat. No. 77-0010>CuFe<sub>2</sub>O<sub>4</sub> – Copper Iron Oxide for x = 0.25, 0.50 and 0.75 samples and
- (iii) Cat. No. 77-0010>CuFe<sub>2</sub>O<sub>4</sub> – Copper Iron Oxide for x = 1.0 sample.

XRD patterns showed the formation of cubic structure with dominant peak corresponding to (311) reflection indicating that the crystallites were preferentially oriented along (311) plane. The lattice parameters were evaluated by using crystal utility of the equation of  $\frac{\sin^2 \theta}{(h^2 + k^2 + l^2)} = \frac{\lambda^2}{4a^2}$  where  $\theta$  is the diffraction angle ( $^\circ$ ), (hkl) is the miller indices,  $\lambda$  is the wavelength of incident X-ray ( $\text{\AA}$ ) and  $a$  is the lattice parameter of the samples ( $\text{\AA}$ ). The observed lattice parameters and evaluated lattice parameters are tabulated in Table 1. Figure 6 shows the variation of the lattice parameters of the Cu<sub>x</sub>Co<sub>1-x</sub>Fe<sub>2</sub>O<sub>4</sub> ferrites with increase in Cu concentration. The lattice parameters were found to be varied with increase in Cu concentration. Muthurani, S. et. al. (2010) has reported that the lattice parameters of the Co-ferrite, Cu-Co ferrite and Cu ferrite are 8.381  $\text{\AA}$ , 8.372  $\text{\AA}$  and 8.370  $\text{\AA}$  respectively [Muthurani, et.al. (2010)]. In this work, the obtained lattice parameters are found to be agreed with the data of Muthurani, S. et. al. (2010).

The crystallite sizes of the samples were estimated by using the Scherrer formula,

$$D = \frac{0.9\lambda}{B \cos \theta}$$

where D is the crystallite size (nm),  $\lambda$  is the wavelength of incident X-ray ( $\text{\AA}$ ),  $\theta$  is the diffraction angle of the peak under consideration at FWHM ( $^\circ$ ) and B is the observed FWHM (radians). The breadth of the Bragg peak is a combination of both instrument and sample dependent effects. To decouple these contributions, it is necessary to collect a diffraction pattern from the line broadening of a standard material such as silicon to determine the instrumental broadening. In this work, the instrumental effects on the breadth of the Bragg peak neglected.

In the present work, the FWHM of the strongest peak (I = 100%) of (311) planes of the XRD patterns were used to calculate the crystallite size and the estimated crystallite sizes of Cu<sub>x</sub>Co<sub>1-x</sub>Fe<sub>2</sub>O<sub>4</sub> samples. The obtained crystallite sizes are also presented in Table 1. It indicates the nanosized Cu-Co ferrites materials. Variation of the crystallite sizes with increase in Cu concentration is shown in Figure 6.

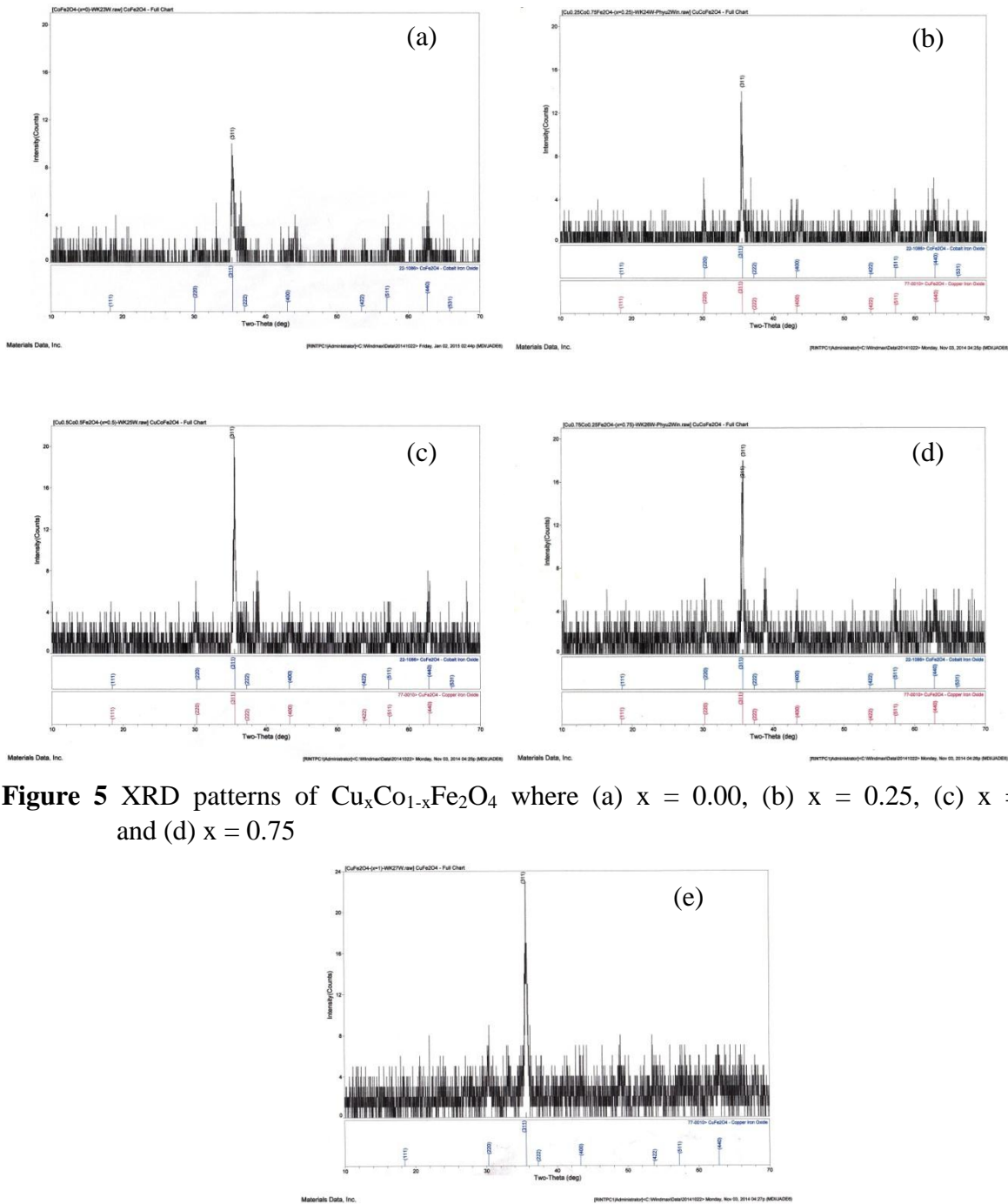


**Figure 5** XRD patterns of  $Cu_xCo_{1-x}Fe_2O_4$  where (a)  $x = 0.00$ , (b)  $x = 0.25$ , (c)  $x = 0.50$ , and (d)  $x = 0.75$

**Figure 5 (e)** XRD pattern of  $Cu_xCo_{1-x}Fe_2O_4$  where  $x = 1.00$

**Table 1** The observed and calculated lattice parameters and crystallite sizes of  $Cu_xCo_{1-x}Fe_2O_4$  samples

Sample (Contents x of Cu)	Obs. $a=b=c$ (Å)	Cal. $a=b=c$ (Å)	D (nm)
0.00	8.4063	8.4063	38.42
0.25	8.3596	8.3596	70.08
0.50	8.3601	8.3601	43.44
0.75	8.3463	8.3464	46.61
1.00	8.3472	8.3574	31.36

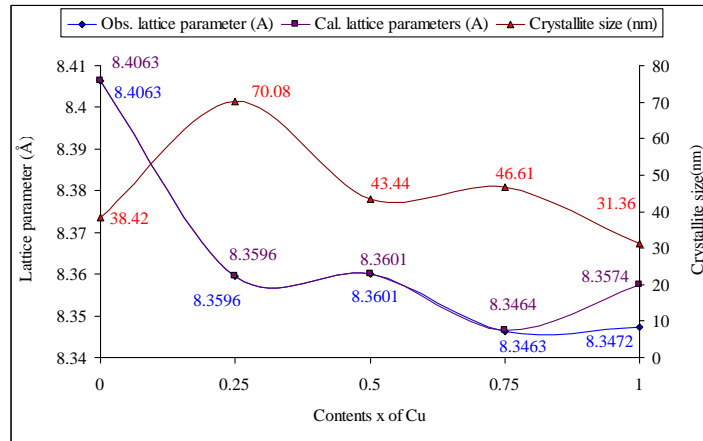


**Figure 6** Variations of the observed and calculated lattice parameters with increase in concentration of Cu and the crystallite sizes with the increase in concentration of Cu of  $Cu_xCo_{1-x}Fe_2O_4$

### SEM Analysis

Due to the microstructure has a major role in the performance of a ceramic sensor, in this work, the microstructures of the end products by SEM to investigate the external morphology of grain shape, size and pore formation of the as-prepared ferrite samples. SEM micrographs of the  $Cu_xCo_{1-x}Fe_2O_4$  samples are shown in Figures 7(a – e). As shown in Figure 7(a), the grain shape of the  $x = 0.00$  sample is block shape in which large intergranular porosities are found. The grain sizes are obtained as in the range of  $0.20 \mu m - 1.20 \mu m$ . In Figure 7(b), the grain shape of  $x = 0.25$  sample is block shape. A few and small intergranular porosities are found and the obtained samples composed of agglomerated particles with poor grain boundary. The grain sizes are obtained as in the range of  $0.10 \mu m - 0.80 \mu m$ . In Figure 7(c) of  $x = 0.50$  sample, the stone like block shape grains are found and they can be clearly seen as non-homogeneous with some holes. The grains sizes are obtained as  $2.50 \mu m - 20.00 \mu m$ . A few intergranular porosities are found with clear grain boundary. As depicted in Figures 7(d) and (e) of  $x = 0.75$  and  $x = 1.00$  samples, the stone like block shape grains are also found with clear grain boundary. A few and small intergranular porosities are also found in the micrographs. The grain sizes are obtained as in the range of  $2.20 \mu m - 18.50 \mu m$  for  $x = 0.75$  and  $1.80 \mu m - 22.50 \mu m$  for  $x = 1.00$ . The obtained grain sizes are listed in Table 2.

In the observed SEM micrographs, there are intergranular porosities due to the decomposition of starting materials (nitrates). According to literature, grain size and pore structure have a major effect on the properties in polycrystalline materials.

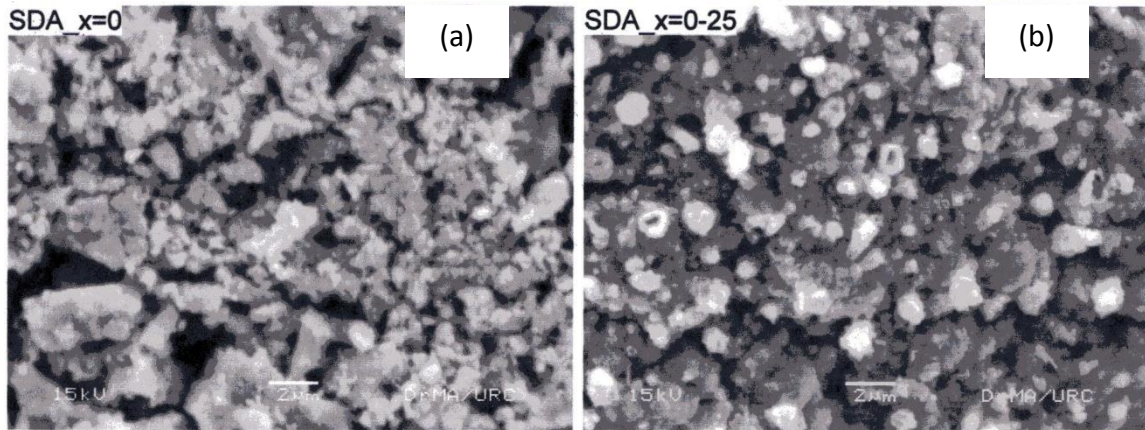


**Figure 7** SEM micrographs of  $\text{Cu}_x\text{Co}_{1-x}\text{Fe}_2\text{O}_4$  where (a)  $x = 0.00$  and (b)  $x = 0.25$

### Humidity Sensitive Electrical Resistance Study

The spinel ferrites are chemically stable, have porous structure and resistive type. This type of property of the materials can be used as humidity sensors applications. In the present work, humidity sensitive electrical resistances  $R$  of the samples in the relative humidity range of 50 RH% – 99 RH% with the step of 1 RH% were observed to examine the change in electrical resistance with increased in humidity. Variations of the electrical resistances  $R$  vs. relative humidity RH% of the samples in the whole relative humidity ranges of 50 – 99 RH% are shown in Figures 8(a – e).

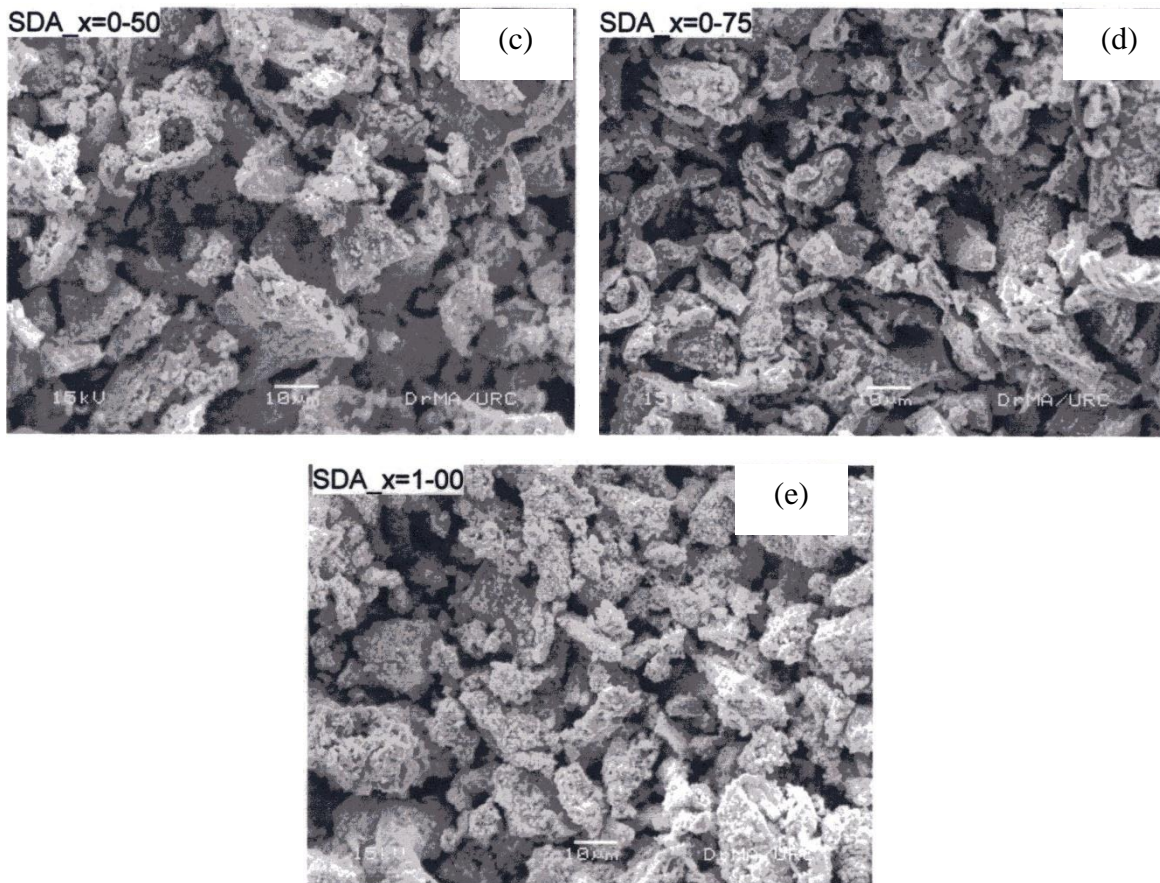


**Figure 7** SEM micrographs of  $\text{Cu}_x\text{Co}_{1-x}\text{Fe}_2\text{O}_4$  where (c)  $x = 0.50$ , (d)  $x = 0.075$  and (e)  $x = 1.00$

**Table 2** The grain sizes of  $\text{Cu}_x\text{Co}_{1-x}\text{Fe}_2\text{O}_4$  samples

Sample (Contents x of Cu)	Grain size ( $\mu\text{m}$ )
0.00	0.20 – 1.20
0.25	0.10 – 0.80
0.50	2.50 – 20.00
0.75	2.20 – 18.50
1.00	1.80 – 22.50

The electrical resistance of the samples decreased with increase in relative humidity. In each of the R vs. RH% graph, it was clearly seen that the change in electrical resistances

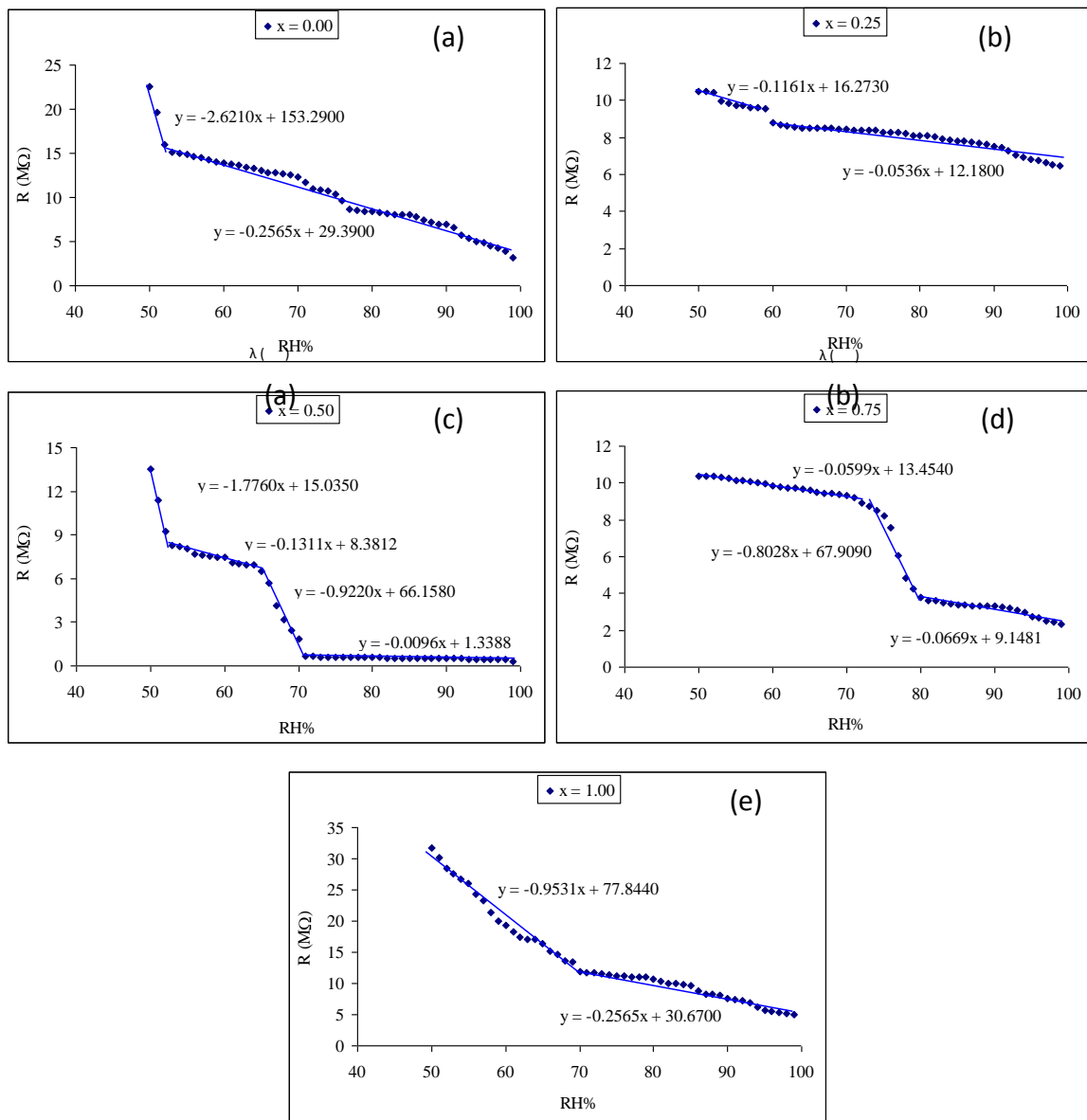


**Figure 8** Humidity sensitive electrical resistance graphs of  $\text{Cu}_x\text{Co}_{1-x}\text{Fe}_2\text{O}_4$  where (a)  $x = 0.00$ , (b)  $x = 0.25$ , (c)  $x = 0.50$ , (d)  $x = 0.75$  and (e)  $x = 1.00$

with relative humidity or slopes of the curves in the R vs. RH% graphs are generally two portions, three portions and four portions with the corresponding humidity ranges. It can be explained as the resistance of the sensing materials slightly decreased because the water molecule is not only physically absorbed in the active group of the ferrites but also can be polarized. The effect can generate space charge and dipoles, and then accumulate and degenerate between electrodes.

In this work, detail variations of the decreased changes in electrical resistances with the corresponding relative humidity ranges or slopes of the R vs. RH% graphs are also presented in Figures 8(a – e). The obtained changes in electrical resistances with the corresponding humidity ranges are tabulated in Table 3.

It was obviously that the changes in electrical resistances with relative humidity or slopes of the R vs. RH% graphs of  $x = 0.00$  (pure  $\text{CoFe}_2\text{O}_4$ ),  $x = 0.25$  ( $\text{Cu}_{0.20}\text{Co}_{0.75}\text{Fe}_2\text{O}_4$ ) and  $x = 1.00$  (pure  $\text{CuFe}_2\text{O}_4$ ) are found to be in two regions. The four step slopes are found in the R vs. RH% graph of  $x = 0.50$  ( $\text{Cu}_{0.50}\text{Co}_{0.50}\text{Fe}_2\text{O}_4$ ). The three step slopes are found in the R vs. RH% graph of  $x = 0.75$  ( $\text{Cu}_{0.75}\text{Co}_{0.25}\text{Fe}_2\text{O}_4$ ). The decreased changes in electrical resistances with relative humidity or slopes of the R vs. RH% graphs of the samples varied with increased in concentration of Cu on the  $\text{Cu}_x\text{Co}_{1-x}\text{Fe}_2\text{O}_4$ .

**Table 3 Change in electrical resistances with the corresponding relative humidity ranges of the  $\text{Cu}_x\text{Co}_{1-x}\text{Fe}_2\text{O}_4$  samples**

Sample (Contents x of Cu)	Slope ( $\text{M}\Omega/\text{RH}\%$ )	Humidity range (RH%)
x = 0.00	2.6210	50 – 53
	0.2565	54 – 99
x = 0.25	0.1161	50 – 59
	0.0536	60 – 99
x = 0.50	1.7760	50 – 53
	0.1311	54 – 64
	0.9220	65 – 71
	0.0096	72 – 99
x = 0.75	0.0599	50 – 72
	0.8028	73 – 80
	0.0669	81 – 99
x = 1.00	0.9531	50 – 70
	0.2565	71 – 99

The sensitivity factor of a humidity sensor can be generally evaluated as follow:

$$S = R_{\text{initial RH}\%} / R_{\text{final RH}\%} = R_{50\text{RH}\%} / R_{99\text{RH}\%}$$

where S is the sensitivity factor,  $R_{\text{initial RH}\%}$  is the resistance at initial relative humidity and  $R_{\text{final RH}\%}$  is the resistance at final relative humidity. In this work, the sensitivity factors of  $\text{Cu}_x\text{Co}_{1-x}\text{Fe}_2\text{O}_4$  humidity sensors are obtained as the followings:

$$S_{x=0.00} = (R_{50\text{RH}\%})_{x=0.00} / (R_{99\text{RH}\%})_{x=0.00} = 22.61 \text{ M}\Omega / 3.18 \text{ M}\Omega = 7.11$$

$$S_{x=0.25} = (R_{50\text{RH}\%})_{x=0.25} / (R_{99\text{RH}\%})_{x=0.25} = 10.49 \text{ M}\Omega / 6.46 \text{ M}\Omega = 1.62$$

$$S_{x=0.50} = (R_{50RH\%})_{x=0.50} / (R_{99RH\%})_{x=0.50} = 13.51 \text{ M}\Omega / 0.32 \text{ M}\Omega = 42.10$$

$$S_{x=0.75} = (R_{50RH\%})_{x=0.75} / (R_{99RH\%})_{x=0.75} = 10.38 \text{ M}\Omega / 2.34 \text{ M}\Omega = 4.44$$

$$S_{x=1.00} = (R_{50RH\%})_{x=1.00} / (R_{99RH\%})_{x=1.00} = 31.68 \text{ M}\Omega / 5.05 \text{ M}\Omega = 6.28$$

The sensitivity factor of the  $x = 0.50$  ( $\text{Cu}_{0.50}\text{Co}_{0.50}\text{Fe}_2\text{O}_4$ ) is the largest one among the investigated samples. It shows that the  $x = 0.50$  sample is the most suitable for the application of humidity sensing material.

### Conclusion

Copper-Cobalt ferrites,  $\text{Cu}_x\text{Co}_{1-x}\text{Fe}_2\text{O}_4$  (where  $x = 0.00, 0.25, 0.50, 0.75$  and  $1.00$ ) were successfully prepared by auto-combustion method. Structural, microstructural and humidity sensitive electrical resistance of the samples were studied in this work. XRD patterns reveal that the samples analogous to cubic structure. The lattice parameters and crystallite sizes varied alternatively with increase in concentration of Cu. SEM micrographs showed that the grain shape and grain sizes varied with the concentration of Cu. The intergranular porosities appeared in each of the SEM micrograph and the samples composed of agglomerated particles. Experimental results from the humidity sensitive electrical resistances measurements showed that the electrical resistances decreased with increase in relative humidity. The changes in electrical resistances of the samples were examined from R vs. RH% graphs. Furthermore, the sensitivity factor of the  $x = 0.50$  ( $\text{Cu}_{0.50}\text{Co}_{0.50}\text{Fe}_2\text{O}_4$ ) was the largest one among the investigated samples. It showed that the  $x = 0.50$  sample was the most suitable for the application of humidity sensor.

### Acknowledgements

We express our gratitude and appreciation to Professor Dr Pho Kaung, Rector, University of Yangon (UY), for his providing necessary research facilities in UY and keen interest for this work. The authors would like to acknowledge Professor Dr Tun Khin, Acting-Rector (Rtd.), University of Yangon (UY) and Professor Dr Myint Kyi, Principal, Hinthada Degree College, for their stimulated suggestions to prepare this paper.

The authors would like to acknowledge Professor Dr Khin Khin Win, Head of Department of Physics, University of Yangon, for her valuable suggestion and comments for this work. The authors would like to thank Professor Dr San San Wai, Head of Department of Physics, Loikaw University, for her kind permission to carry out this work.

### References

- Ahmad, I. & Farid, M.T. (2012). Characterization of Cobalt Based Spinel Ferrites with Small Substitution of Gadolinium. *World Applied Sciences Journal*, 19, 464–469.
- Fawzi, A.Z., Sheikh, A.D. & Mathe, V.L. (2010). Structural, Dielectric Properties and AC Conductivity of  $\text{Ni}_{(1-x)}\text{Zn}_x\text{Fe}_2\text{O}_4$  Spinel Ferrite. *Journal of Alloys and Compounds*, 502, 231–237.
- Maria1, K.H., Choudhury, S. & Hakim, M.A. (2013). Structural phase transformation and hysteresis behavior of Cu-Zn ferrites. *International Nano Letters*, 3, 1–10.
- Praveena, K., Sadhana, K. & Murthy, S. R. (2013). Elastic behaviour of Sn doped Ni-Zn ferrites, *International Journal of Scientific and Research Publications*, 3, 1–4.
- Rezlescu, N., Rezlescu, E., Popa, P. & Tudorache, F. (2002). ON THE HUMIDITY SENSITIVITY OF A CERAMIC ELEMENT. STRUCTURE AND CHARACTERISTICS. *Journal of Institute of Technical Physics*, 8, 89–97.
- Sharma, R.K., Suwalka, O., Lakshmi, N., Venugopala, K., Banerjee, A. & Joy, P.A. (2005). Synthesis of Chromium Substituted Nano Particles of Cobalt Zinc Ferrites by Co-precipitation. *Materials Letters*, 59, 3402–3405
- (2011). *The Humidity/Moisture Handbook*, Machine Applications Corporation.